2003 Pacific Conference on Earthquake Engineering

Seismic displacement response predictions using a calibrated substitute structure approach

M.R. Edwards, J.L. Wilson, & N.T.K. Lam

Department of Civil and Environmental Engineering, The University of Melbourne, Australia.

ABSTRACT: Performance based design of structural systems requires realistic predictions of displacement response to earthquake excitation. Considerable research effort has been undertaken internationally with approximate methods published to enable practitioners to make some prediction of peak displacement demand. This paper describes some of the research that has been undertaken to examine the nature of deformation and damping in reinforced concrete frame systems based on a large data base of experimental testing with a particular focus on the substitute structure method. The findings have been incorporated into detailed time history analysis models that have, in turn, been used to calibrate a linear idealisation of response. Comparisons made with other published predictive methods have been encouraging for the limited structural range considered. The results suggest that a substitute structure methodology can be calibrated to provide an improved prediction of maximum displacement response when compared with other published methods.

1 INTRODUCTION

In recent years displacement based seismic evaluation and design of structures has attracted much research interest. Observations made of the performance of structures in large earthquakes has in part prompted this interest. Survivability is observed to be more influenced by displacement capability than lateral strength. Further, at serviceability response levels, non-structural damage to architectural components is largely related to drift. Consequently, reliable predictions of displacements at several limit states are required to assess expected structural performance.

Time history analysis (THA) is generally considered to be a reliable displacement prediction method, but is very analysis intensive. More simplified procedures which provide reasonable predictions are often required. For the structural assessment of existing buildings both ATC-40 (1997) and FEMA 273 (1997) provide methodologies for predicting the maximum displacement response due to a given demand spectrum. These predictions can be compared to an assessment of the displacement capability of the structural system and conclusions drawn.

Research work has been undertaken at the University of Melbourne to refine the existing ATC-40 predictive method based on the substitute structure idealisation (Shibata and Sozen 1976). Tools are being developed to both quantify displacement demand and to assess the deformation capacity of reinforced concrete special moment resisting frame (SMRF) systems dominated by first modal response. Displacements for the calibration process were determined using THA models in which both the pre and post-yield damping has been incorporated hysteretically Results are presented herein for a single degree of freedom (SDOF) type frame and comparisons between the predictions of several simplified methods and the benchmark THA results are made.

2 SIMPLIFIED PREDICTIVE METHODS

The Coefficient Method of FEMA 273 represents a refinement of the equal displacement observation

of Newmark and Hall. Recent research has improved the average predictions made with special attention given to the short period equal energy regime and P/delta effects. Despite these refinements the approach continues to predict inelastic displacements from the nominally elastic period part of the spectrum with considerable scatter persisting.

ATC-40 uses the Capacity Spectrum approach proposed by Freeman (1998). The structural period of a substitute linear system is progressively adjusted with the damping and damped elastic spectra updated using Newmark and Hall's adjustment relationships. Convergence is achieved when the updated spectra and an adaptation of the structures pushover curve intersect at the adjusted period. This method focuses on the portion of the spectra associated with inelastic response, but requires a calibrated damping model to represent the real hysteretic damping mechanisms.

One further approach is to use inelastic spectra, as described by Chopra (Chopra et al 1999), in which the hysteretically damped response of real structures is directly incorporated into the spectra. Uncertainties are associated with the spectral factors used to generate inelastic spectra that are based on simplifications of the structures hysteretic behaviour. Furthermore there is a need for a consistent definition of yield from which system ductilities are calculated.

3 DEFINITIONS OF DUCTILITY

Structural ductility can be defined in three basic ways; curvature ductility, rotational ductility, and global displacement ductility. Curvature ductility is mainly associated with adequate sub-assemblage performance, whereas rotational ductility reflects the aggregated contributions of the plastic hinge region to inelastic hinge rotation. In this research rotational ductility has been utilised as a measure of both the inelastic demand and the deformation capacity of component hinges. Rotational ductility was evaluated using the deformation model described below, and THA models permitted the global displacement ductilities of frame systems to be subsequently determined.

The rotational ductility was associated with a hinge region assumed to be comprised of the beam/column joint and the portion of the member extending 1.8 times its depth from the face of the transverse framing member. Rotational deformations were the aggregate of joint shear distortion, reinforcement strain penetration, and hinge flexural curvature. Shear deformations were treated separately. The point of "yield" was defined at first tensile yield, or when the extreme concrete compression strain reaching 0.2%, whichever was encountered first.

Global ductility was determined from the pushover curve of the generalised SDOF system using a bi-linear approximation, with the area under the bi-linear curve matched to the area under the real pushover curve. Post ultimate maximum displacement capacity was defined as that associated with a 20% loss of strength over 4 cycles, or 50 % strength loss in any hinge of the frame system.

4 SUBASSEMBLAGE DEFORMATION MODEL

A deformation model was required for the individual sub-assemblages that make up the system to assign deformation capacity to hinge regions and to relate hinge behaviour to frame response. The principal deformation components identified, modelled and calibrated against experimental data were:-

1. Flexure
2. Shear
3. End rotation due to reinforcement strain penetration
4. Beam\column joint shear distortion

The curvature distribution of the framing member was evaluated with moment/curvature software and used to determine flexural rotations and deformations. The Bernoulli assumption of plane sections remaining plane was made, but corrections were applied for post-yield conditions as described below.

Park and Paulay's (Park and Paulay 1975) model for shear distortions was used up to yield. The model's shear stiffness was locally reduced for post-yield behaviour where non-closing flexural/shear cracks form and stirrups yield to accommodate hinge region rotations.

The bar development model proposed by Alsiwat (Alsiwat et al 1992) was adopted to evaluate rotation at the face of transverse framing members due to strain penetration into beam/column joints. Rotation was assumed to occur about a constant neutral axis depth. The clamping effects of column axial loads on beam column joints were addressed using bond accentuation relationships determined by Soroushian (Soroushian et al 1991).

The monotonic joint shear distortion was determined using a simplified model proposed by Bonacci (Pantazoupolou and Bonacci 1992) with corrections applied for post-yield cyclic behaviour. Experimental work suggested a dependency of post-yield joint shear stiffness on rotational ductility demand. Relationships were regressed from the data that modify Bonacci's monotonic joint shear stiffness as rotational ductility demand increases beyond unity.

Post-elastic cyclic response differs from monotonic as it is very loading history dependent. The Bernoulli assumption is no longer valid as diagonal shear cracks form and link with flexural cracks. The uncorrected deformation model as described above is a close match to monotonic loading behaviour but provides only an upper bound envelope to the degraded hysteresis loops of cyclic. The difference between the deformation model and the cyclic envelopes was addressed empirically rather than mechanistically. For member hinges the collective rotational distortions were modelled as a combined spring possessing piecewise linearities. Parameters were derived from experimental data to assign stiffnesses to the combined spring up to ultimate and to reflect the strength degradation beyond.

The predicted yield load deflections were calculated and compared to the experimental results to check the overall validity of the combined deflection model. In Figure 1 the results from 27 beam hinges of 24 specimens tested by 9 different researchers are compared. On average the match is satisfactory although some scatter is observed.

5 **NATURE OF STRUCTURAL DAMPING**

Structural damping as a key displacement response parameter was examined and quantified using the same set of experimental data used for the deformation model. Distributed pre-yield damping was examined separately to the post-yield damping which is concentrated in hinge regions. In the post yield regime shear damping mechanisms for beams were uncoupled from the flexural mechanisms. For all regimes the area method was used for assigning an equivalent viscous damping (EVD) level. In making this selection, the need to adjust the reference values obtained to optimise displacement prediction accuracy was acknowledged and addressed. Key findings are discussed below.

5.1 *Pre-yield global damping*

Within the pre-yield range there are no discrete hinges formed. Energy absorption is distributed throughout the members, being more pronounced in regions of high moment. The global behaviour of the system was quantified for the study of sub-yield damping. By focussing on the location for first yield, the damping obtained was related to the maximum moment normalised by that which would induce yield. The results obtained from seven sub-assemblage specimens tested at several amplitudes of pre-yield displacement are presented in Figure 2. The gradual increase of damping with moment amplitude is consistent with a system that is gradually becoming more inelastic, and the value of 7% at yield compares favourably with published values in the literature.

5.2 *Post-yield shear damping*

Beyond yield, damping is concentrated in plastic hinge regions. More extensive frame hinging imparts greater ductility and damping to the system. Hinge shear damping was investigated separately for beams as non-closure of flexural cracks and stirrup yield can result in significant shear mechanism development. Low aspect ratio beams particularly exhibit lower overall damping due to a larger

portion of the system deflection being associated with shear, and due to high shear stresses that are associated with lower levels of shear damping. The beam hinge shear damping mechanism was evaluated using continuously monitored shear distortion test data. The shear damping level at a rotational ductility of 1.0 was assumed equal to the system sub-yield damping at yield. The shear damping behaviour for high and low shear stress levels is presented in Figure 3.

5.3 *Post yield flexural damping*

Flexural damping was determined by deducting the hinge shear response and that of the beam outside the hinge region from the observed overall experimental behaviour of the beam element. By deducting the energy absorption and strain energies of these from the corresponding global values the residual strain energy and damping associated with the flexural damping mechanism was calculated. For column hinges the shear and flexural damping mechanisms were left combined. The results obtained for SMRF type beam hinges are presented in Figure 4. Damping was found to increase sharply following flexural yield and the total data was found to be grouped based on typical rotational ductility step size.

6 **DETAILED TIME HISTORY ANALYSIS MODEL**

A single degree of freedom reinforced concrete frame was designed and an inelastic model of the frame generated for damping calibration purposes using Ruaumoko. The deformation and damping models already described were utilised to obtain a frame that would as closely as possible exhibit the behaviour of the real frame, were it constructed and tested. Significantly the damping of frame elements was incorporated hysteretically at all response amplitudes, consistent with experimental observations. This work is described below.

6.1 *Single storey structural design*

The two storey reinforced concrete building used for calibration responded essentially as a single degree of freedom system due to the presence of a steel framed upper floor. It was designed using IBC 2000 and ACI-318 for Californian seismicity. A one-way pre-cast floor system resulted in seismic loading dominance for the ductile frames. Fixed base columns were assumed with no foundation compliance contributing to displacement capability and system damping. The ductile mechanism was side-sway with column hinging at both top and bottom.

6.2 *Sub-assemblage modelling*

The deformation and damping behaviour of each column and each beam sub-assemblage from transverse member face to point of inflection was matched to model the overall response of the frame system. This was achieved using an elastic framing member with multiple end springs. The arrangement for a beam member is illustrated in Figure 5.

Three rotational stiffness degrading bi-linear springs were used to match inelasticity and damping in the pre-yield regime. These progressively yielded with increasing response from 20% of the yield moment upwards. Shear deformation and damping in the hinge zone was modelled separately using a single transverse spring having Sina type hysteresis. Finally, for additional post-yield flexibility and damping, two rotational Modified Takeda strength degrading springs were used that permitted a separate definition of both the negative and positive cyclic envelopes. Spreadsheets were developed to evaluate the associated 42 parameters needed for the Ruaumoko model.

6.3 *Single storey THA model*

Each sub-assemblage was modelled (as per Section 6.2) using damping values associated with large rotational ductility step sizes. Having modelled the sub-elements, these were assembled into a non-linear model for analysis using Ruaumoko. The final model was comprised of some 68 inelastic

springs.

All sub-yield damping was represented by hysteretic elements for the cyclic pushover model used to obtain the global damped behaviour. This was varied for the model used for earthquake THA work in which 1% Rayleigh type damping was substituted with the balance hysteretically incorporated.

6.4 *Single storey global response*

A global yield displacement of 38.7mm (1% drift approx) was determined from a monotonic pushover analysis using the definition in Section 3. The frame was then subjected to a cyclic pushover both in the pre-yield and at post-yield displacement ductility steps of 1.0. The damping values obtained using the area method can be seen in Figure 6.

7 **CALIBRATION**

The reference damping curve presented in Figure 6 was adjusted to optimise prediction accuracy using the inelastic THA model and a suite of filtered earthquake records.

7.1 *Methodology*

The calibration procedure was as follows:-

1. Subject the model to a sequentially amplified record of each earthquake ground motion to induce progressively increasing displacement response.
2. Determine the maximum displacement response and the secant period at that point.
3. From a family of DRS for the ground motion, determine by scaling and interpolation which equivalent viscous damping level for the equivalent linear system would have matched the displacement. This is illustrated in Figure 7.
4. Determine the damping correction factor λ that would adjust the area method value at that ductility level to the value that would match the displacement
5. Regress the collective λ value set for all ground motions to optimise displacement prediction accuracy for the system at all amplitudes of response.

7.2 *Earthquake selection*

Accelerograms from seven well-known earthquakes recorded at stiff to intermediate soil sites were selected and DC filtered. Soft sites records with distinct soil resonance effects were not chosen nor ground motions with pulse type effects (near field). Large events were chosen so as to have a frequency content similar to the ultimate design event.

Two additional artificial ground motions were included for comparative purposes, generated using Simqke to match the IBC spectra for site flexibilities B and D. These site categories bounded the site flexibilities of the calibration earthquakes.

7.3 *Damping correction factor*

A total of 14 damping correction factors for each of the 7 natural ground motions were used. The correction factors obtained are presented in Figure 8. Considerable scatter was noted, even for a given earthquake. The λ values followed the erratic undulations of the ADRS plot for each event. The bi-linear regression of the λ data indicated that the EVD values based on the area method needed to be reduced by 28% across the post-yield range. The corrected damping curve is presented on Figure 6.

It was postulated that synthetic ground motions would provide a smoother set of λ value data as large ADRS undulations would not be present. This was found to be the case as indicated in Figure 8 by comparing the λ values for the synthetic and real earthquake records.

7.4 *Comparison with other methods*

Maximum displacement responses were predicted for each amplified earthquake record (126 total) using the FEMA 273 Co-efficient Method. For the calibration structure the method condenses down to the equal displacement observation. The benchmark response of the detailed THA model was divided by the predicted value from the co-efficient method and is plotted in Figure 9 against overall global ductility. As can be seen, the scatter is considerable with a tendency on average to under-predict displacements. In some instances actual displacements were found to be double the prediction.

The ATC-40 method was also employed using the Type B hysteresis damping relationship and Newmark and Hall's relationships for adjusting spectra for changes to damping. The results are presented in Figure 10. It can be seen that in the pre-yield ATC-40 over-predicts displacements due to the assumption of 5% damping. For moderate post-yield ductilities it typically under-predicts, with actual displacements exceeding predictions by over 50%.

Inelastic spectra were also generated using the elasto-plastic spectral factors proposed by Chopra (Chopra et al 1999). The results in Figure 11 show that the mean prediction accuracy and scatter obtained using the spectra are similar to those obtained using the Coefficient Method as both methods are based on similar premises.

Finally, using the bi-linear λ relationship determined above, and Freeman's (1998) Capacity Spectrum approach, displacement predictions were made. Newmark and Hall's spectral adjustment relationships for damping were used and the results are presented in Figure 12. The prediction accuracy is more consistent across the full range of ductile response and typically the actual response rarely exceeded the prediction by more than 30%.

8 **DISCUSSION**

The provision of simple but accurate tools for displacement prediction is challenging. Ground motions exhibit great variability making prediction scatter inherent to any predictive method. Fundamentally there is a problem in trying to represent a non-linear hysteretic system with a linear viscously damped system. For this reason a linear substitute structure can have only limited success.

The FEMA 273 Co-efficient Method, while giving a reasonable average prediction, has great scatter. Actual response may be double that predicted. The recommendation by Whittaker (Whittaker et al 1998) to increase predictions by 50% to upper-bound actual responses is supported by this limited study.

The ATC-40 Type B hysteresis damping curves were a close match to the uncalibrated area method curves obtained for the single storey frame (Fig. 6). The observed trends in prediction accuracy with global ductility demand could be reduced by optimising the assignment of damping by the method. Prediction accuracy is further improved if elastic spectra are generated using THA routines.

The work undertaken has in effect been an optimisation of the substitute structure method, and the results have been encouraging. Accuracy has been achieved for both serviceability and ultimate limit states, which would be improved if elastic spectra from THA were used rather than empirical factors. The predictable λ value trends for the synthetic ground motions have suggested that the capacity spectrum approach could be made very reliable for code smoothed spectra, offsetting the need for Newmark and Hall type damping adjustment factors. Unique damping curves could potentially be generated for a range of typical structural frame types and soil conditions using the methodology presented, thereby permitting the designer to make more accurate displacement predictions.

9 **CONCLUSION**

The work presented demonstrates that a substitute structure methodology can be calibrated to provide an improved prediction of maximum displacement response when compared to other published methods.

10 ACKNOWLEDGEMENT

The work reported in this paper forms part of a project investigating displacement based methods in earthquake eng. funded by the Australian Research Council (Grant Nos A89701689 and 589711277).

REFERENCES:

Alsiwat J.M. and Saatcioglu M. 1992, Reinforcement anchorage slip under monotonic loading, *Journal of Structural Engineering, ASCE*. 118(9). 2421-2438.

Applied Technology Council 1997, Recommended Methodology for Seismic Evaluation and Retrofit of Buildings, Redwood City, California.

Chopra A.K. and Rakesh K.G. 1999, Capacity–demand-diagram methods for estimating seismic deformation of inelastic structures : SDF systems, *PEERC*, Report No. PEER-1999/02.

Federal Emergency Management Agency 1997, NEHRP Guidelines for the Seismic Rehabilitation of Buildings, FEMA 273, October.

Freeman S.A. 1998, The capacity spectrum method as a tool for seismic design, *Proc of 11th European Conference on Earthquake Engineering*.

Pantazopoulou S. and Bonacci J. 1992, Consideration of questions about beam-column joints, *ACI Structural Journal*. 89(1). 27-36.

Park R and Paulay T. , 1975, Reinforced concrete structures", Wiley.

Shibata A. and Sozen M.A. 1976, Substitute-structure method for seismic design in R/C, *Journal of Structural Engineering, ASCE*. 102(ST1). 1-18.

Soroushian P. and Choi K. 1991, Analytical Evaluation of Straight Bar Anchorage Design in Exterior Joints", *ACI Structural Journal*. 88(2). 161-168.

Whittaker A. , Constantinou M. and Tsopelas P. 1998, Displacement estimates for performance-based seismic design, *Journal of Structural Engineering, ASCE*. 124(8). 905-912.

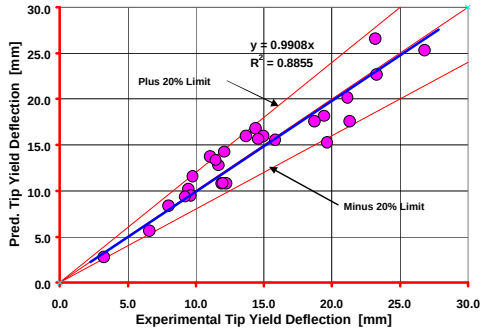

Figure 1 Beam Deflection Match at Yield

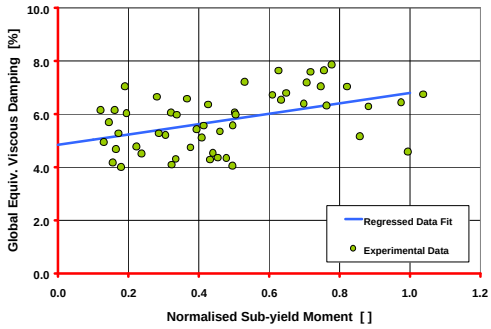

Figure 2 Hysteretic Sub-yield Damping

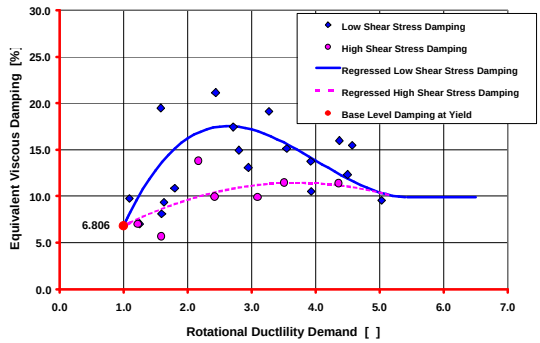

Figure 3 Beam Shear Damping

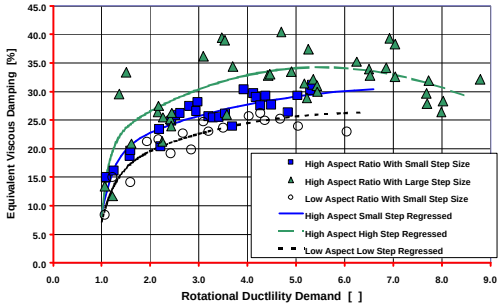

Figure 4 Beam Flexural Damping

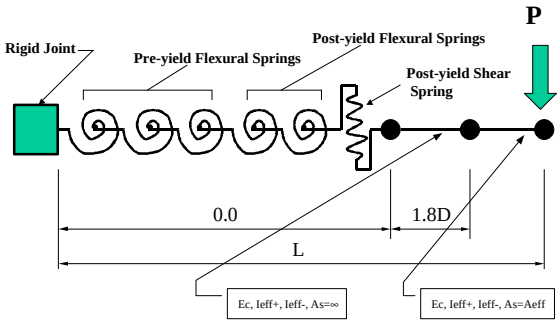

Figure 5 Beam Hinge Composite Springs

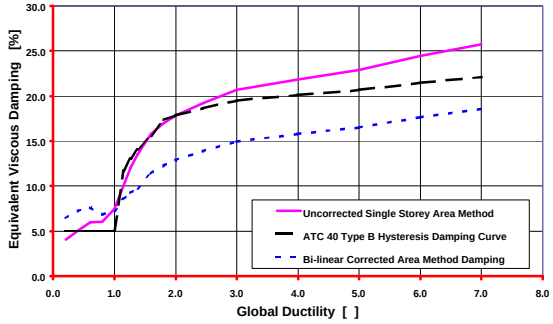

Figure 6 Single Storey Structure Global Damping Curves.

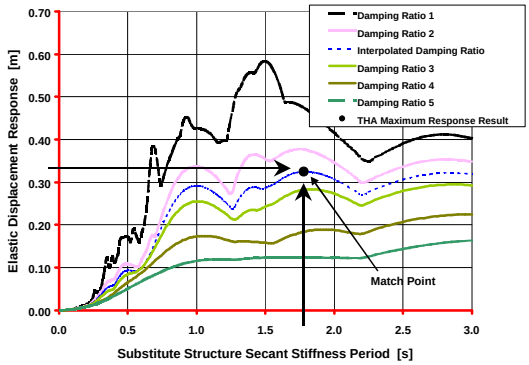

Figure 7 Calibration Method

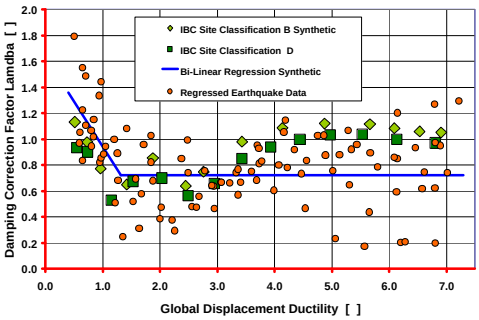

Figure 8 Correction Factor l Data Regression

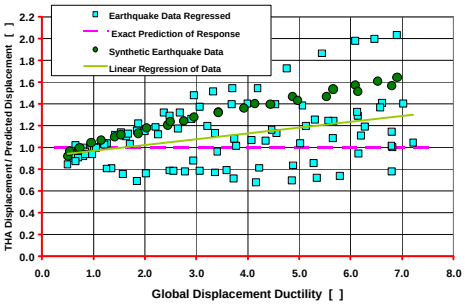

Figure 9 FEMA 273 Prediction Results

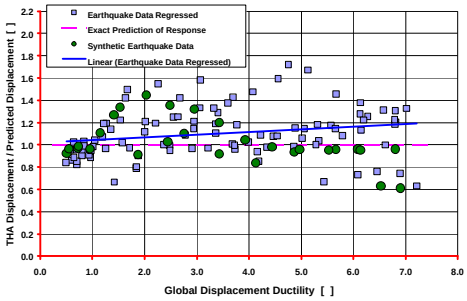

Figure 10 ATC-40 THA Prediction Results

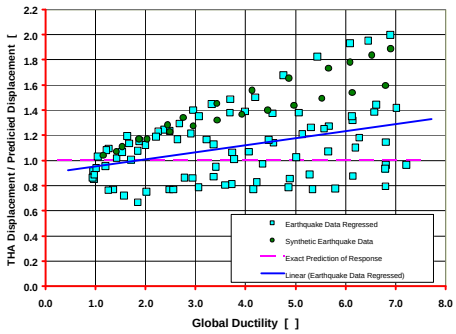

Figure 11 In-elastic Spectra Prediction Accuracy

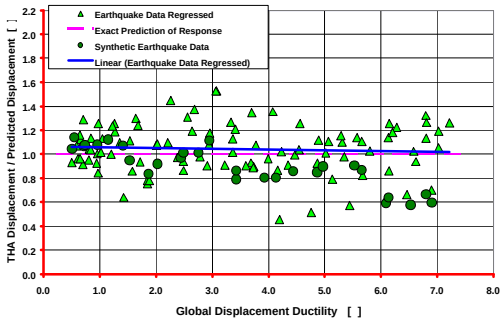

Figure 12 Calibrated Substitute Structure Prediction Accuracy